Author(s): Lechner, Lorenz G. & Wu, Fan & Danneau, Romain & Andresen, Sören E. & Hakonen, Pertti J.

Title: rf-electrometer using a carbon nanotube resonant tunneling transistor

Year: 2010

Version: Final published version

Please cite the original version:

Lechner, Lorenz G. & Wu, Fan & Danneau, Romain & Andresen, So?ren E. & Hakonen, Pertti J.. 2010. rf-electrometer using a carbon nanotube resonant tunneling transistor. Journal of Applied Physics. Volume 107, Issue 8. 084316/1-3. ISSN 0021-8979 (printed). DOI: 10.1063/1.3387927

rf-electrometer using a carbon nanotube resonant tunneling transistor

Lorenz G. Lechner, Fan Wu, Romain Danneau, Søren E. Andresen, and Pertti Hakonen

Citation: Journal of Applied Physics **107**, 084316 (2010); doi: 10.1063/1.3387927
View online: http://dx.doi.org/10.1063/1.3387927
View Table of Contents: http://scitation.aip.org/content/aip/journal/jap/107/8?ver=pdfcov
Published by the AIP Publishing

rf-electrometer using a carbon nanotube resonant tunneling transistor

Lorenz G. Lechner,[1,a)] Fan Wu,[1] Romain Danneau,[1] Søren E. Andresen,[2] and Pertti Hakonen[1]
[1]*Low Temperature Laboratory, Helsinki University of Technology, FI-02015 HUT, Finland*
[2]*Niels Bohr Institute, University of Copenhagen, 2100 København Ø, Denmark*

(Received 8 January 2010; accepted 10 March 2010; published online 30 April 2010)

We have studied resonant tunneling transistors (RTT) made of single-walled carbon nanotube quantum dots in the Fabry–Pérot regime. We show sensitivity to input charge as high as $5 \times 10^{-6}\ e/\mathrm{Hz}^{1/2}$ with a carrier frequency of 719 MHz at 4.2 K. This result is comparable to the best values of charge sensitivity so far reported for radio frequency single electron transistors (rf-SET). Unlike SETs, whose operating temperature is limited as Coulomb blockade vanishes as $1/T$, a RTT can operate at higher temperatures, since the dephasing length $l_\phi \propto 1/T^{2/3}$. © *2010 American Institute of Physics*. [doi:10.1063/1.3387927]

I. INTRODUCTION

The precise measurement of electric charge and charge fluctuations has tremendous importance in metrology and beyond. In order to achieve sensitivities of mere fractions of the charge quantum the devices of choice have been relying on charge quantization effects: the best results were measured using single-electron transistors (SET) or their faster counterpart the radio-frequency transistor (rf-SET). The rf-SET being the advanced implementation[1] that overcomes the bandwidth limitations of the SET by using high frequency matching circuits. This matching enables the readout of the real part of the SET impedance using conventional microwave techniques without sacrificing charge sensitivity.

Unfortunately rf-SETs require a tradeoff between temperature range and performance in terms of gain-bandwidth product. The sensitivity is maximized when the device is operated in the strong instead of the weak tunneling regime, where cotunneling is dominant over sequential tunneling.[2] Then energy sensitivity is expected to approach $0.5\hbar$ and larger bandwidths can be achieved due to lower usable Q-factors. However, the effective Coulomb energy diminishes rapidly with lowering resistance R_T of the tunnel barriers, eventually limiting the operating temperature.[3] For this reason devices not operating based on Coulomb blockade principles are desirable.

Quantum dots in the Fabry–Pérot regime are one of these alternatives. They exhibit resonant tunneling through discrete energy levels due to size quantization effects. Similar to strong tunneling SETs they also show enhanced charge sensitivity due to shot-noise suppression as the transmission is close to $T \sim 1$.[4] And like SETs they benefit from carbon nanotubes as building material. Electron interference patterns have already been studied in single-walled carbon nanotubes.[5] But while single-wall carbon nanotubes have been used extensively to fabricate rf-SETs[6–9] no nanotube rf-devices based on resonant tunneling transistors (RTTs) have been demonstrated so far. Owing to their low impedance, these Fabry–Pérot transistors might be the best choice when the largest bandwidth is desirable.

II. EXPERIMENT

Our device consists of a single wall carbon nanotube (SWNT) contacted by metal electrodes and controlled by a top-gate. The tubes were grown from prepatterned catalyst islands by chemical vapor deposition (CVD) in an Ar, H_2, and CH_4 atmosphere at ≈900 °C.[10] Pairs of 25/15 nm Ti/Au electrodes with 0.3 μm spacing were defined between the catalyst islands by electron beam lithography. A central 25 nm thick Ti top-gate, 0.1 μm wide, was deposited between the contacts. The insulating barrier was created by five Al layers, each oxidized 2 min in ambient atmosphere. In a final step a Cr/Au mask with 230 μm square bond pads was deposited. To reduce parasitic capacitances that would limit the rf-operation an insulating (sapphire) substrate was used [see Fig. 1(a) for a side view of the sample layout]. The sample was connected to an LC-circuit, formed by the inductance $L=150$ nH of a surface mount inductor and the bond-wires, and the parasitic capacitance $C=0.3$ pF of the bond pads.

A surface mount bias-tee was used to couple the dc bias and rf-signal. The top-gate was connected to a separate coaxial line for high-bandwidth modulation. Before detection the signal was amplified using a home-made low-noise amplifier with a frequency range of 600–950 MHz.[11] The entire setup was immersed in liquid helium for cooling to 4.2 K. The rf-output was detected in a fashion dependent of the goal of the measurement such as: (1) by a spectrum analyzer to investigate the carrier modulation spectra or (2) by mixer demodulation for homodyne detection at a particular frequency.[9]

III. RESULTS AND DISCUSSION

Figure 2(a) shows the differential conductance dI/dV_{ds} versus gate voltage V_g and drain-source bias voltage V_{ds}. The device shows a pronounced dI/dV_{ds} modulation pattern that is periodic in V_g. The conductance varies between 0.6 and 1.4 e^2/h $(=G_0)$. The absence of strong blockade regions in-

a)Author to whom correspondence should be addressed. Electronic mail: lorenz.lechner@ltl.tkk.fi.

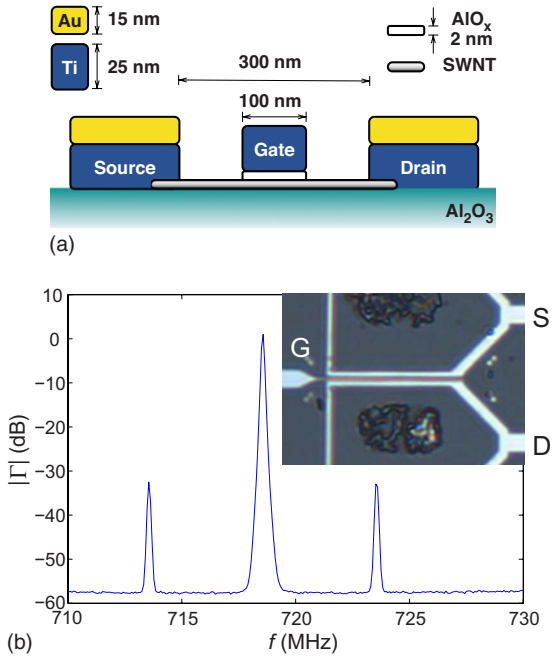

FIG. 1. (Color online) (a) Layout side view of the bias leads and gate electrode connected to the single walled nanotube. (b) Spectrum of the reflection signal using 5 MHz modulation of 0.04 e(rms) at the gate. The charge sensitivity is calculated from the side peak SNR; their root-mean-square amplitude in comparison with the noise floor of the preamplifiers. The carrier power −63 dB m defines the reference level (0 dB). The inset displays an optical image of the sample ($\sim 15\times 10$ μm^2): leads D, G, and S denote drain, gate, and source electrodes, respectively.

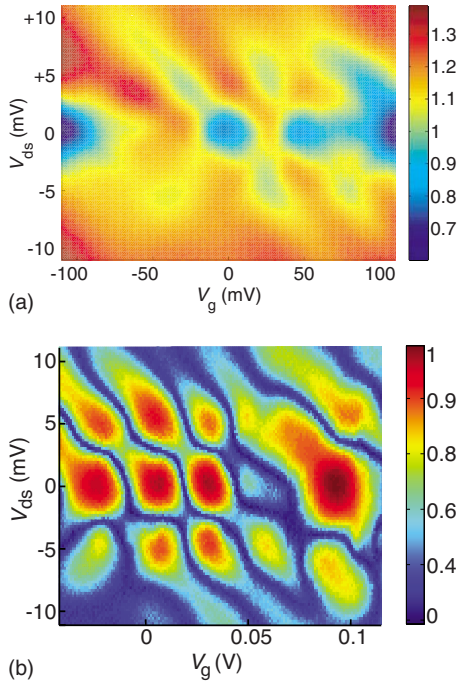

FIG. 2. (Color online) (a) Measured two-dimensional (2D)-map of the differential conductance dI/dV_{ds} in units of e^2/h (color scale on the right) as a function of gate voltage V_g and bias voltage V_{ds}. (b) 2D-map of the charge sensitivity as a function of gate voltage V_g and bias voltage V_{ds} calculated from SNR. Color bar on the right denotes $\delta q_{opt}/\delta q$, the inverse charge sensitivity $1/\delta q$ scaled with the inverse optimum sensitivity of $(\delta q_{opt})^{-1}$ $=(5\times 10^{-6}\ e/\sqrt{\text{Hz}})^{-1}$.

dicates that our quantum dot is not in the Coulomb blockade regime. In addition to the zero-bias pattern, there are also conductance modulations around $V_{ds}=\pm 5$ mV identifying the Fabry–Pérot nature of the interference pattern. Similar low conductance Fabry–Pérot behavior has been reported for example in Ref. 12. The level spacing in our sample corresponds to the size quantization with $L=0.3$ μm.[5] By using the phase shift formula $\pm((eV/\hbar v_F)l_{tube}+(\pi/4)\times(l_{tube}C_LV_g/e))$ with $v_F=8\times 10^5$ m/s, the observed gate period of 70 mV (see Fig. 2) agrees with $C_g=l_{tube}C_L=6.4$ aF within 10% accuracy. This value is by a factor of 2 larger than what we typically obtain for similar gate configuration of samples with Coulomb blockade.[8] Since this difference cannot arise from quantum capacitance (i.e., density of states) differences, it has to be related to the quality of Al_xO_y and its dielectric constant.

In radio-frequency measurements, the optimum operating point was found by searching for points of perfect matching, i.e., vanishing reflection at the resonance frequency $f_0=718.6$ MHz. The signal was homodyne detected by mixer, and the phase was tuned to be sensitive only to the real part of the RTT impedance. Using a spectrum analyzer, the input carrier power was tuned to obtain maximum signal-to-noise ratio (SNR) of the sidebands at $f_0\pm f_{mod}$, while keeping on a 1.0 mV_{rms} gate-voltage modulation at $f_{mod}=5$ MHz [Fig. 1(b)]. We find the largest zero-bias SNR $\text{SNR}_{max}=25.2$ dB at gate voltage $V_g=0.095$ V [Fig. 2(b)]. In terms of gate charge, the reference AC-signal corresponds to $q_{\text{ref}}=0.04$ e(rms). This value allows us to derive a charge sensitivity of $\delta q_{\text{rms}}=(q_{\text{ref}}/\sqrt{2BW}10^{\text{SNR}/20})=5\times 10^{-6}\ e/\sqrt{\text{Hz}}$, where $BW=10^5$ Hz is the resolution bandwidth of the measurement, and the factor $\sqrt{2}$ accounts for the fact that there are two side peaks.[9] Even though our result falls short of the best nanotube[8] and nanowire[13] results, it beats the recently obtained rf-SET sensitivities in silicon devices.[14,15]

Figure 2(b) also displays clear SNR peaks off zero bias indicating that our device can also work well under finite-bias conditions. Using a dc bias of 5 mV the sensitivity was, on average, only degraded by a factor of 10% to 15% compared to the zero bias value. Notice that the gate-period of the sensitivity pattern in Fig. 2(b) is half of the conductance pattern of Fig. 2(a), which indicates that the device functions equally well at positive and negative slopes of $G(V_g)$.

The temperature dependence of the gate modulation was studied in a separate cooldown. Although the total resistance of the device had grown a bit higher the Fabry–Pérot pattern stayed qualitatively unchanged. Similar to Liang *et al.*[5] we observe dI/dV_{ds} dips predominantly. The dips become less pronounced with increasing temperature but signature features of the interference pattern continue to be visible up to 23 K. This fact allows us to establish a lower limit for the phase coherence length $l_\varphi\sim l_{tube}=300$ nm at 23 K. The related phase coherence time τ_φ is governed by processes with small energy transfer; electron–electron collisions, or, analogously, interactions of electrons with electromagnetic fluctuations. For a one-dimensional conductor the temperature dependence of the intrinsic dephasing length is given by $l_\varphi \propto T^{-2/3}$.[16] In order to investigate the temperature dependence of the charge sensitivity, $\delta V/\delta I - V_g$-curves were recorded for temperatures $9\leq T\leq 23$ K in a separate cool down. For a

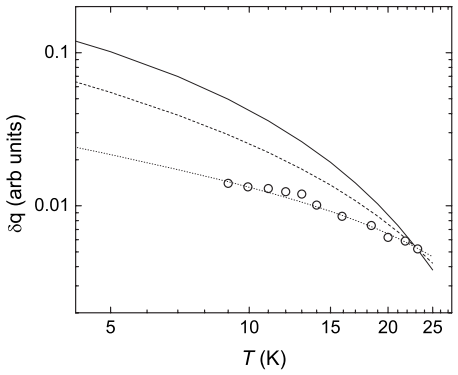

FIG. 3. Charge sensitivity δq vs temperature T at V_g=91 mV. The curves illustrate the calculated dependence from Eq. (1) using $l_\varphi \propto T^{-\beta}$ with β=1 (solid), β=2/3 (dashed), and β=1/3 (dotted). Charge sensitivity of the Fabry–Pérot interferometer thus vanishes slower than $1/T$ in Coulomb blockade based devices.

device in the Fabry–Pérot regime, the gradient $\delta R_d/\delta V_g$ of the curves is proportional to the charge sensitivity, when the device works at optimum matching. Figure 3 shows the evolution of the resistance gradient with temperature T for V_g =91 mV, where maximal SNR was obtained. To analyze this temperature dependence quantitatively, we employ the basic double-barrier quantum dot model with phase coherent transport.[17] This model yields for the transmission at energy E

$$T_L(E) = \frac{T_l T_r}{1 - 2\sqrt{R_l R_r}\exp(-2\alpha l_{tube}) + R_l R_r \exp(-4\alpha l_{tube})}, \quad (1)$$

where T_l, T_r, R_l, and R_r are transmission and reflection probabilities of the left and right contacts, respectively, $\alpha = 1/l_\varphi$ is the attenuation of phase coherence per unit length,[17] and the phase picked up per one round trip in the dot has been taken as a multiple of 2π. In order to match the average transmission of our sample, we estimate T_l=0.8 and T_r=0.3. Consequently, we obtain l_φ=350 nm at 23 K in order to match the measured "contrast" of $G(V_g)$ modulation. A comparison of the model to the measured results in Fig. 3 is done using three different temperature dependencies for dephasing time $\tau_\varphi \propto 1/T^\beta$: $\beta = 1, 2/3, 1/3$. The exponent β=1/3 is found to agree best to the data although β=2/3 should be theoretically the correct dependence. One explanation for this discrepancy would be diffusive instead of ballistic transport inside the nanotube. In this case the dephasing length is given by $l_\varphi = (D\tau)^{0.5}$ instead of $l_\varphi = v_F\tau$. This discrepancy could mean that the transport through our tube is not fully ballistic or that there are extrinsic dephasing mechanisms present; most likely thermal fluctuations in the metallic gate.[18] In every case, we may conclude that the charge sensitivity of the Fabry–Pérot interferometer vanishes slower than $1/T$ which is the asymptotic behavior for devices based on Coulomb blockade.[19]

Extrapolation of l_φ for our sample to T=4.2 K yields l_φ=0.62 μm using β=1/3. Our result compares well to findings reported in literature that are normalized to T =4.2 K. We find our phase coherence length two times larger than values obtained for other CVD grown SWNTs, e.g., l_φ=0.3 μm at T=4.2 K reported by Liang *et al.*[5] Using β=2/3 for extrapolation, we get l_φ=1.1 μm, which is comparable to the largest value l_φ=1.6 μm reported for a semiconducting SWNT by Javey *et al.*[20]

IV. CONCLUSION

We have shown RTT operation of a SWNT quantum dot in the Fabry–Pérot regime. The demonstrated charge sensitivity of 5×10^{-6} $e/\mathrm{Hz}^{1/2}$ is comparable to the best values reported for carbon nanotube rf-SETs (Ref. 8) and for nanowire rf-electrometers.[13] This result was obtained at 4.2 K and, according to our modeling, it can be further improved by cooling the device. In comparison with Coulomb blockaded nanotube devices, the operation of carbon nanotube Fabry–Pérot transistors may persist up to higher temperatures in samples where the ratio of l_{tube}/l_φ is small.

ACKNOWLEDGMENTS

We wish to thank P. E. Lindelof, and B. Placais for fruitful discussion. This work was supported by the EU under Contract No. FP6-IST-021285–2. L. Lechner acknowledges funding from the Emil Aaltonen foundation.

[1] R. Schoelkopf, P. Wahlgren, A. Kozhevnikov, P. Delsing, and D. Prober, Science **280**, 1238 (1998).
[2] D. V. Averin, *Macroscopic Quantum Coherence and Quantum Computing* (2001), p. 399.
[3] X. Wang, R. Egger, and H. Grabert, Europhys. Lett. **38**, 545 (1997).
[4] Y. Blanter and M. Buttiker, Phys. Rep. **336**, 1 (2000).
[5] W. Liang, M. Bockrath, D. Bozovic, J. H. Hafner, M. Tinkham, and H. Park, Nature (London) **411**, 665 (2001).
[6] M. J. Biercuk, D. J. Reilly, T. M. Buehler, V. C. Chan, J. M. Chow, R. G. Clark, and C. M. Marcus, Phys. Rev. B **73**, 201402(R) (2006).
[7] Y. Tang, I. Amlani, A. Orlov, G. Snider, and P. Fay, Nanotechnology **18**, 445203 (2007).
[8] S. E. S. Andresen, F. Wu, R. Danneau, D. Gunnarsson, and P. J. Hakonen, J. Appl. Phys. **104**, 033715 (2008).
[9] L. Roschier, M. Silanpää, W. Taihong, M. Ahlskog, S. Iijima, and P. Hakonen, J. Low Temp. Phys. **136**, 465 (2004).
[10] J. Kong, H. T. Soh, A. M. Cassell, C. F. Quate, and H. Dai, Nature (London) **395**, 878 (1998).
[11] L. Roschier, Cryogenics **44**, 783 (2004).
[12] W. Liang, M. Bockrath, and H. Park, Annu. Rev. Phys. Chem. **56**, 475 (2005).
[13] H. A. Nilsson, T. Duty, S. Abay, C. Wilson, J. B. Wagner, C. Thelander, P. Delsing, and L. Samuelson, Nano Lett. **8**, 872 (2008).
[14] S. J. Angus, A. J. Ferguson, A. S. Dzurak, and R. G. Clark, Appl. Phys. Lett. **92**, 112103 (2008).
[15] M. Manoharan, Y. Tsuchiya, S. Oda, and H. Mizuta, Nano Lett. **8**, 4648 (2008).
[16] B. Altshuler, A. Aronov, and D. Khmelnitsky, J. Phys. C **15**, 7367 (1982).
[17] S. Datta, *Electronic Transport in Mesoscopic Systems* (1997).
[18] F. Guinea, Phys. Rev. B **71**, 045424 (2005).
[19] We assume that we remain in the short sample limit where l_φ still exceeds l_{tube}.
[20] A. Javey, J. Guo, Q. Wang, M. Lundstrom, and H. Dai, Nature (London) **424**, 654 (2003).